In: Proc of the Int. Conf. "Impacts of Fuel Quality on Power Production", EPRI report No. 1014551 (2007), pp.7-61 to 7-76, EPRI (Ed.), Palo Alto, CA; USA

Development, test and application of a new low-pressure impactor for particle sampling at high temperatures up to about 1,000°C

T. Brunner [a,b,c,*], J. Friesenbichler [a], I. Obernberger [a,b,c], A. Berner [d]

[a] Institute for Resource Efficient and Sustainable Systems, Graz University of Technology, Inffeldgasse 21b, A-8010, Graz, Austria;

[b] Technical University of Eindhoven, Department of Mechanical Engineering, Section Process Technology, Den Dolech 2, P.O. Box 513, 5600 MB Eindhoven, the Netherlands;

[c] Austrian Bioenergy Centre GmbH, Inffeldgasse 21b, 8010 Graz, Austria;

[d] Institute of Experimental Physics, University of Vienna, Strudlhofgasse 4, A-1090 Vienna, Austria;

* corresponding author
e-mail: thomas.brunner@tugraz.at; Tel.: + 43 316 48130013; Fax: +43 316 4813004

Abstract

Information concerning aerosols already present in the hot furnace before entering the convective path of biomass combustion units offers highly valuable insights into aerosol and deposit formation processes. To gain this information an impactor that can operate in-situ at temperatures up to about 1,000°C has been developed, manufactured as well as subsequently tested and evaluated. The results of this research work are presented in this paper. With this new particle sampling device it is possible to gain information about particle size distribution and concentration of aerosols sampled at high temperatures directly in the furnace. Furthermore, the chemical composition, shape and structure of the particles can subsequently be investigated by wet chemical as well as SEM/EDX analyses. The results achieved by measurements with the new impactor are of great relevance for an improved knowledge about aerosol formation processes, deposit formation processes and an appropriate aerosol and deposit formation model development. The high-temperature impactor has already proven its applicability during several field tests at pilot-scale as well as large-scale biomass combustion and biomass and coal cofiring plants. In this paper the detailed design of the impactor is firstly described and then results gained during test runs at a waste wood fired large-scale CHP plant are presented. Detailed information concerning the particle size distribution, concentration, chemical composition and the shape of aerosols sampled in the boiler and the convective path have thereby been gained and are finally applied to describe the aerosol formation process during waste wood combustion.

Keywords: high temperature particle sampling, impactor, aerosol formation, particle size distribution, biomass combustion

Nomenclature:

C	Cunningham slip correction factor
C_d	contraction coefficient
c_p	heat capacity at constant pressure
C_v	velocity loss factor
D	particle diameter
D_j	equivalent diameter of the jet
D_o	equivalent diameter of the orifice
K_n	Knudsen number
N	number of orifices
P	pressure at the point of observation
P_j	pressure in the free jet leaving the orifice
P_u	pressure upstream of the critical orifice, in a stagnant flow region
P_i	pressure in an inter-stage region upstream of the orifices
PSD	particle size distribution
R_i	specific gas constant
T	temperature
T_a	temperature upstream the critical orifice, in a stagnant flow region
T_j	jet temperature
T_i	temperature in an inter-stage section

U_f fluid velocity
U_j jet velocity
V volume of 1kg mass of the fluid
V_j volumetric flow rate of the jet at Tj, Pj
W_j jet width
η viscosity of the fluid
κ ratio of specific heats
ρ particle density

1 Introduction

Within the last years considerable data and experiences concerning aerosol and fly ash formation processes during biomass combustion could be gained. This knowledge is based on data which represent the initial point (fuel characterization) as well as the end point (aerosol emissions) of the processes related to particle formation. The most relevant factors influencing aerosol formation can be deduced from these results. The data for instance show, that the chemical composition of the fuel respectively the release of easily volatile compounds from the fuel influence the mass of aerosols formed during the combustion process. It is also already well known, that processes such as nucleation, condensation and coagulation determine the final particle size distribution of aerosol emissions at boiler outlet. However, especially the behavior of not easily volatile compounds such as Ca which are also found in the aerosol fraction demands for further investigations. Moreover, with respect to deposit formation and corrosion in the convective boiler sections, also the question, if nucleation and condensation processes take place even in the hot zones of the furnace or in the boiler, are of relevance. Therefore, mathematical modeling of the aerosol formation process could be an appropriate tool. However, to verify the models measurement data from upstream the convective path are needed. To gain appropriate data, an unique impactor that can operate at temperatures up to about 1,000°C has been developed, manufactured as well as subsequently tested and evaluated in the frame of the EU-funded project "BIOASH" – the high-temperature low-pressure impactor (HT-LPI).

In this paper comprehensive information concerning the HT-LPI development is given. The HT-LPI concept is outlined and as an example for its operation, measurement results gained during test runs at a combustion plant utilizing waste wood as fuel are presented.

2 Objectives

The main objective of the research work was to develop a particle sampling and measurement device that can be operated at temperatures up to 1,000°C. With this device it should be possible to determine the particle size distribution (PSD) and concentration of aerosols (particles < 1 µm aerodynamic diameter) in the flue gas. Moreover, a possibility for subsequent chemical analyses of the particle samples should be given.

The design should avoid the condensation of vapors during sampling which would impact the measurement results. Moreover, the sampling and measurement device should be applicable at different sections of a combustion plant without the need for major constructive changes. Therefore it should be designed for the utilization at openings and measurement ports which are usually available at combustion plants (e.g. inspection glasses, SNCR additive injection ports, etc.).

The particle sampling device developed should be manufactured and tested. Moreover, the validation of the basic concept and subsequently the check of its applicability for high temperature particle sampling and measurement as well as its utilization during test runs at different combustion plants in order to investigate aerosol formation formed a main objective of the work.

3 Literature review

With state-of-the-art particle measurement equipment it is not possible to determine the particle size distribution, concentration and chemical compositions of aerosols in the hot flue gas. However, certain research and development activities dealing with particle sampling from the hot flue gas have already been performed.

Jimenez, Ballester (2005) performed a comparative study of different methods for the sampling of high temperature combustion aerosols. An aerodynamic quenching particle sampling (AQPS) probe, a N_2-dilution probe as well as a thermophoretic sampling probe have been used for particle sampling in the flue gas of a laboratory-scale entrained flow reactor burning Orujillo (residues of the olive oil production process). Samples were taken at gas temperatures from 560°C to 1,300°C. The authors concluded that the use of the AQPS probe resulted in the formation of very fine particles (~15 nm) by nucleation of the inorganic vapors. The main artifact introduced by the dilution probe was the condensation of KCl, which results in high amounts of this compound at any temperature. Therefore, the authors considered the use of this probe inappropriate for the study of particle formation processes in the presence of condensable species. The results of tests performed with the

thermophoretic sampling probe showed that also this probe can introduce significant artifacts because of nucleation and/or condensation of vapors.

Strand et al. (2004) designed and experimentally examined a sampling method for high-temperature aerosols from biomass combustion, in which nucleation and condensation from fly ash forming vapors is controlled. The sampling method includes a high-temperature dilution probe in which the sampled gas is diluted and then cooled. Laboratory tests using a model aerosol with known concentrations of SiO_2 particles and KCl vapor showed effective separation of the KCl vapor from the aerosols by deposition on the probe walls when using a high dilution ratio. With a lower dilution ratio the KCl vapor generated a distinct nucleation mode when cooled in the probe.

Dixkens, Fissan (1995) developed a ceramic-cascade-impactor for size classified particle sampling in high pressure- and high temperature-(HPHT) processes, which normally are coal-dust gasification or pressurized fluidized bed combustion of coal. The ceramic-cascade impactor is situated in an electrically heated pressurized housing outside of the HPHT-process where the same temperature and pressure as in the HPHT-process itself can be obtained. Therefore, nucleation or condensation of vapors is prevented. The impactor has been successfully tested at temperatures < 900°C and pressures < 12 bar. The cut diameters of the three stages of the ceramic-cascade impactor are 5 µm, 3 µm and 1 µm. A drawback of ceramic materials is the possibility of reactions with ash forming vapors which is especially of relevance for biomass combustion systems.

4 Methodology approach

In order to reach the objectives mentioned, the new sampling and measurement device was based on a low-pressure impactor concept. In contrary to the extractive methods using a cooled probe, the HT-LPI is situated directly in the furnace. The hot flue gas is sucked through the impactor within a residence time of 0.15 s (at an operation temperature of 1,000°C). Because the HT-LPI is pre-heated in the furnace for a certain period of time, a cooling of the flue gas and consequently nucleation or condensation of vapors in the HT-LPI should not occur.

Compared to the above mentioned ceramic-cascade impactor, the cut diameters of the HT-LPI also cover the sub-micron range (down to about 30 nm) and therefore it is designed to provide valuable information concerning aerosol formation.

The development of the high-temperature low-pressure impactor (HT-LPI) is based on the common design of a Berner-type low-pressure impactor (BLPI). To keep the costs within the bounds of economic possibilities only standard materials were used for the manufacturing of the HT-LPI. To check the validity of the results obtained from measurements with the HT-LPI, a comparison with BLPI measurements under cold gas conditions has been performed. Finally, the HT-LPI was applied during test runs at real-scale combustion units. By analyzing the particle samples taken during these test runs by SEM/EDX, again a verification of the main design parameters was possible.

5 Development of the HT-LPI

5.1 BASIC CONCEPT

As already mentioned the HT-LPI was developed based on the common design of a BLPI. The BLPI as well as the HT-LPI are working on the same principle. Flue gas is sucked through the impactor. In the impactor the flue gas is forced to change flow direction for several times. This is realized by a number of subsequent impaction stages each consisting of an orifice plate, a spacer ring and a stagnation plate (see Figure 1). Particles which are too large as to follow the changing flow direction between the orifice plate and the stagnation plate are precipitated on a sampling foil placed on the stagnation plate. The cut diameter of each stage is defined by the volumetric flow rate through the impactor, the number and diameter of identical orifices and the distance between the orifice plate and the stagnation plate. In the sequence of the stages the number and diameter of the orifices as well as the distance between the orifice plate and the stagnation plate are changed stage by stage in a way that the typical cut diameter of a stage decreases.

The HT-LPI consists of 8 stages. A critical orifice downstream of the last impaction stage controls flue gas flow through the impactor. The impactor is covered with an inner casing where it is fixed by a strong spring in order to avoid leakages. The inner casing is then inserted into an outer casing which is finally placed in the flue gas flow.

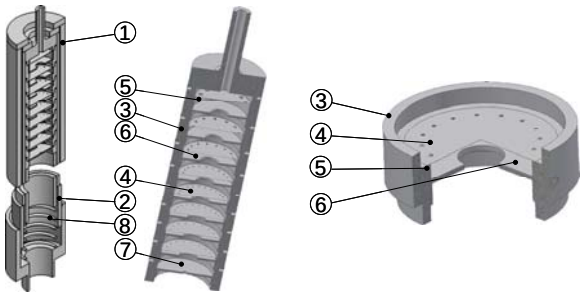

Figure 1: Basic design of the HT-LPI

Explanations: 1 … outer casing, 2 … inner casing, 3 … shell, 4 … orifice plate, 5 … spacer ring, 6 stagnation plate, 7 … critical orifice, 8 … spring

5.2 MATERIALS

A main problem during the development of the HT-LPI was the high operation temperature which requires special materials. High temperature resistant materials are not easily available and usually not easily machinable. Dixkens, Fissan (1995) used the technical glass-ceramic MACOR for the development of a ceramic-cascade impactor. Since the maximum continuous operation temperature of MACOR is only 800°C the ceramic material would not be applicable for the HT-LPI. Moreover, experiences with first approaches which were based on the utilization of ceramic materials such as SiC have shown that these materials are generally too brittle. Especially at high temperatures even very small forces lead to serious destructions. Therefore, different alloys have been screened concerning their applicability and finally the following materials have been selected.

Heat resisting stainless steel, quality 1.4841 (15 X CrNiSi 25 20) was used for the impactor stages, spacers and stagnation plates as well as for the casings. The steel is applicable for operation temperatures up to 1,120°C. For the 100 µm thick orifice plates Inconell 600, a nickel-chromium alloy with good oxidation resistance at high temperatures and good resistance in chloride containing environments, was used. The orifices were drilled by laser. Stainless steel 1.4841 as well as Inconell 600 have already proven their applicability for these special requirements.

As mentioned, both alloys consist of a considerable amount of Cr. During first high-temperature tests of the HT-LPI a Cr-enrichment in the sampled particles has been identified. Although the amount of Cr found decreased with increasing number of tests performed, Cr was consequently excluded from all evaluations of HT-LPI samples.

In an early phase of the development sampling foils made of a Hastelloy alloy were applied. Hastelloy turned out to be not applicable for sampling foils due to very high weight losses at high temperatures. Even thermal treatment for more than 5 hours did not lead to a constant weight of the foil. After comprehensive testing of different options, platinum was chosen as the most suitable material for the sampling foils.

Due to its high temperature resistance, quartz fiber was chosen as sealing material.

5.3 DESIGN OF THE HT-LPI

It was agreed to drill the thin orifice plates by laser. This technique however is expected to produce rather large differences in axial and radial shape of the orifices, especially with increasing diameters. It would then be difficult to determine by microscopy the effective aperture diameter of the aperture. With thin orifices the individualities are expected to become less important because of a better optical definition of the size and the shape of the aperture. Also losses of kinetic energy by friction are rather small for thin orifices.

5.3.1 Flow through the orifices

The orifice plates are 100 µm thick. The diameters of the orifices are 315 µm (nominal size) in stage #01 and equal or larger in the upper stages. The thickness of the plates are therefore 1/3 in terms of the orifice diameter and less (see Table 1). In such thin orifices the jets detach from the edge of the apertures and contract within a rather short distance from the aperture. Consequently, the diameters of the aerosol jets impacting on the stagnation plate are smaller than the diameters of the apertures. Practically the contraction coefficient for round orifices, which is the ratio of the area of cross section of the jet to the area of the aperture, is about $C_d = 0.62$ according to literature (Dougherty and Franzini 1977; Bohl 1971). This value quoted for incompressible flow also applies to compressible flow.

For thin apertures of large diameters the velocity loss factors are about $C_v = 0.98$ (Dougherty and Franzini 1977). These factors indicate an adiabatic and rather ideal flow. Pressure drops are almost completely transformed into kinetic energy of the fluid. Losses of kinetic energy produced by the break up of a "vena contracta" inside an orifice, by friction due to velocity profiles in the jet and by contact with the wall can be neglected. Assuming adiabatic, under-critical flow and nearly zero velocities in the inter-stage regions the jet velocity becomes

$$U_j = C_v \cdot \left(\frac{2 \cdot \kappa}{\kappa - 1} \cdot R_i \cdot T_a \cdot \left(1 - \left(\frac{P_j}{P_u} \right)^{\frac{\kappa - 1}{\kappa}} \right) \right)^{0.5}$$

In this equation the term $(\kappa \cdot R_i \cdot T_a)^{0.5}$ is the velocity of sound U_a at the temperature T_a upstream the orifices, and this temperature is equal to the ambient temperature of the impactor according to thermodynamic principles. The equation for the jet velocities becomes therefore

$$U_j = C_v \cdot U_a \cdot \left(\frac{2}{\kappa - 1} \cdot \left(1 - \left(\frac{P_j}{P_i} \right)^{\frac{\kappa - 1}{\kappa}} \right) \right)^{0.5}$$

Jet velocities and all other velocities of the fluid in the impactor are proportional to the sonic velocity at ambient temperature.

The volumetric flow rate of the jets V_j at temperatures T_j and pressure P_j in the jet, becomes

$$V_j = U_j \cdot N \cdot \frac{D_j^{\,2} \cdot \pi}{4} = U_j \cdot N \cdot \frac{D_o^{\,2} \cdot \pi}{4} \cdot C_d$$

5.3.2 The Stokes number

The Stokes number is an essential parameter of impactors. Its critical value at 50% efficiency, STK_{50}, determines the cut size of an impaction stage. As a rule this critical value has about the same value in geometrically similar flow fields. It does not depend on the jet velocity U_j or on the jet width W_j. Regarding compressible flow this rule might not hold.

The Stokes number is a dimensionless number,

$$STK = D^2 \cdot \rho \cdot C \cdot \frac{U_j}{18 \cdot \eta \cdot W_j} = \frac{D^2 \cdot \rho \cdot C}{18 \cdot \eta} \cdot \frac{U_j}{W_j}$$

This formulation is directly derived from the equation of motion and is equivalent to other definitions presented in the literature. The Stokes number is a scaling factor for the motion of a particle in a flow with variable velocities. In the dimensionless equation of motion, $d\upsilon/d\tau = (1/STK) \cdot (\omega - \upsilon)$, the term $d\upsilon/d\tau$ becomes large for $STK \ll 1$. Such particles adjust quickly to a change of the fluid velocity ω. These particles set barely off a stream line. For $STK \gg 1$, $d\upsilon/d\tau$ becomes small and the trajectories of such particles are rather not disturbed by variable velocities. In an impaction stage, particles of $STK \gg 1$ collect on a substrate, whereas particles of $STK \ll 1$ stay in the flow. The Stokes number represents the ratio of two characteristic times, that is, the relaxation time $\tau_r = D^2 \cdot \rho \cdot C/(18 \cdot \eta)$, which the particle needs for adjusting to a disturbed flow, and the duration of the disturbance, $\tau_d = (W_j/U_j)$, which is available for this adjustment.

The Cunningham slip correction factor used in the calculations is given by

$$C = 1 + Kn \cdot \left(1.257 + 0.4 \cdot e^{-\left(\frac{1.1}{Kn} \right)} \right)$$

For incompressible flow there is a large body of critical Stokes numbers available, both experimental and calculated data. For extremely laminar flow the critical Stokes numbers of round orifices can be as small as $STK_{50} = 0.11$. For jets with some turbulence the critical Stokes numbers may rise to about $STK_{50} = 0.125$. These differences are not dramatic. A change by 12% in STK_{50} leads to an increase of the cut off size by about 6% for large particles. In the nanometer size range this increase may amount to 12% for decreasing cut sizes and gas pressures. Interacting jets may bring up the critical Stokes numbers to about $STK_{50} = 0.25$. For the orifice array applied in the HT-LPI, $STK_{50} = 0.125$ is used.

Little is known about critical Stokes numbers in compressible flows at high jet velocities. It can be assumed that the STK_{50} values for incompressible flow can be used, but some problems are to be discussed. In the stagnation region of the impinging jet the fluid undergoes strong variations of temperature and pressure which affect the viscosity η and the slip correction factor C along the path of a particle. So the values of viscosity and slip correction factor used in the critical Stokes number are undetermined averages. Compressibility of the fluid certainly reduces the axial extent of the stagnation region, especially in the vicinity of the point of stagnation. It has been shown however that particles having Stokes numbers close to critical values move near the axis, when entering the region of stagnation, but they impact on the plate off axis, at the end of the region of stagnation. Their deposits form a ring with at a diameter larger than the jet width. It is assumed that this behavior holds both for incompressible and compressible flow. These "critical" particles follow the compression near the point of stagnation and the decompression in the outer regions before being deposited. Consequently, compression of the fluid is not supposed to change the critical Stokes number.

Due to the temperature and pressure changes the slip correction factor and the viscosity vary along the paths of particles. Average values or correction factors for the critical Stokes numbers must be used. When the particles are large, the slip correction factor which is about $C = 1$, is not affected by compressibility. The viscosity however is. For jet velocities of about 250 m/s, the temperature differences experienced by a STK_{50} particle are $\Delta T = 20°C$ to -11.13°C. This corresponds to a viscosity difference of $\Delta\eta = 181.2 – 165.8$. On average the effective viscosity becomes 173.5. With this value instead of the viscosity at ambient temperatures the critical Stokes number would shift to $STK_{50} = 0.120$. The cut diameter would shift by 2% to smaller sizes.

For small particles characterized by $C>>1$ the situation is different. The slip correction factor C and the viscosity η depend both on the mean free path of the gas molecules. They are more or less proportional to this parameter. Considering the ratio C/η, we expect the effects of the mean free path to cancel. So the critical Stokes numbers of compressible flow hold also for high jet velocities. First preliminary investigations of critical Stokes numbers in the regime of high jet velocities support this result (Kröpfl et al. 2003).

For the design of the HT-LPI $STK_{50} = 0.125$ for the velocity range was applied.

5.3.3 Effects of critical orifice on the operational state of the impactor

The critical orifice which is installed at the end of the impactor restricts the volumetric flow aspirated by the instrument, and sets the pressure drops of the individual stages. Two essential points are to be noted. The volumetric flow rate thus controlled depends on ambient temperature only. The ratios of the pressure ahead and downstream the orifices are independent of ambient temperature and ambient pressure.

The critical orifice is operated at critical conditions. By a strong vacuum pump the pressure in the orifice drops to a critical pressure P_c at which the jet flow reaches the velocity of sound. For the orifices specified this limit is not exceeded when the pressure downstream of the orifice falls below the critical pressure. The width of the jet W_j is proportional to the width of the orifice, W_o.

$$W_j = C_c \cdot W_o$$

The contraction coefficient C_c may depend on temperature and pressure, but is expected to vary in narrow limits only. Given the critical temperature T_c the critical pressure P_c in the jet, and the size the volumetric flow rate V_c of the critical jet becomes

$$V_c = \frac{4}{\pi} \cdot W_o^{\,2} \cdot \kappa \cdot R_i \cdot T_c$$

Clearly this critical volumetric flow rate depends on the acoustic velocity. The corresponding volumetric flow rate aspirated by the impactor is given by

$$V_a = V_c \cdot \frac{P_c}{P_a} \cdot \frac{T_a}{T_c}$$

In operation the critical orifice and the stages of the impactor will run under certain conditions. In order to transport the same amount of gas and to match the volumetric flow rates the stages will settle on certain pressures. The most characteristic ones are the inter-stage pressures met in the regions of low velocities between stages. The ratios of these pressures upstream and downstream of the orifices are characteristic for the state of operation. They determine the jet velocities in the stages, and the volumetric flow rates of the jets.

Provided the impactor is operated with a critical orifice, the characteristic pressure ratios do not depend on ambient pressure. A variation of ambient pressure changes the amount of gas to be transported in the impactor, but not the velocities in the impactor, or the corresponding pressure ratios. The characteristic pressure ratios do not depend on ambient temperature. All velocities in the impactor are proportional to the acoustic velocity, so a

change of ambient temperature affects the volumetric flow rates and all velocities in the impactor in the same way.

Changes of pressure ratios are expected to occur in narrow limits when the diverse coefficients the contraction coefficient C_c, the velocity coefficient C_v and the discharge coefficient C_d depend on ambient conditions.

5.3.4 Temperatures and pressures in the cascade impactor

Schematically a stage of the LPI cascade impactor consists of the orifice plate, the distance ring, and the collection plate, all of which are contained in a shell. The fluid has its lowest average velocity upstream of the orifices in the inter-stage regions. It is assumed that the average velocities in these regions are so small that the kinetic energies of the fluid can be neglected, when compared to the kinetic energies of the jets.

It is also assumed that heat fluxes into the impactor are marginal, so the flow is adiabatic. The balance of energy can then be expressed by the simple relation that the enthalpy of the fluid and its kinetic energy are constant within the impactor, at any point of the fluid:

$$H + \frac{U_f^2}{2} = P \cdot V + U + \frac{U_f^2}{2} = Cp \cdot T + \frac{U_f^2}{2} = \text{const.}$$

Assuming that the velocities of the fluid outside the impactor and in the inter-stage regions are practically at zero levels, the kinetic energy of the fluid is neglected. The energy relation yields $c_p \cdot T_a = c_p \cdot T_i$, or the temperatures in the inter-stage region are identical to the ambient temperature ($T_a = T_i$).

The velocities of the jets, U_j, are also derived from this relation. They are given by

$$U_j = 2 \cdot c_p \cdot (T_a - T_j)$$

By the relation for adiabatic changes of state of the ideal gas, the temperatures T_a and T_j are replaced by the pressures in the jet P_j and P_i in the inter-stage region upstream of the orifices:

$$U_j = C_v \cdot \left(\frac{2 \cdot \kappa}{\kappa - 1} \cdot R_i \cdot T_a \cdot \left(1 - \left(\frac{P_j}{P_i} \right)^{\frac{\kappa - 1}{\kappa}} \right) \right)^{0.5}$$

Together with these thermodynamic relations the parameters "aspirated volumetric flow rate", "ambient temperature" and "pressure ratios" are sufficient for calculating the temperatures, pressures and volumetric flow rates of the jets.

5.3.5 Design of the impactor

The design of the impactor follows a step-by-step program. Given the flow rate aspirated by the impactor V_a the properties of the entrance stage are calculated. With the size W_o and the number N_o of orifices the jet velocity U_j and the pressure drop, P_j/Pu, are calculated. The parameters for calculating the velocity are varied until the desired cut size is obtained according to the Stokes number STK_{50}. Ambient pressure and temperature are used for setting the slip correction factor C and the viscosity η. Finally the pressure in the stage and the corresponding volumetric flow rate are calculated. This volumetric flow rate is used in the next step for calculating the properties of the following stage.

The lay-out of the HT-LPI uses assumptions based on the principles discussed above. The main assumptions are.

- The velocities in the impactor are strictly proportional to the acoustic velocity of the ambient medium. Once these velocities are known for a specific state of operation, as fixed by a critical orifice in the exhaust of the impactor, at standard ambient temperature and pressure, the velocities at other than standard conditions multiply by the ratio of acoustic velocities U_a/U_0. This result is independent of the kind of the medium which is assumed to be an ideal gas.
- The ratios of the pressure in a jet to the pressure ahead of the corresponding orifice are independent of ambient temperatures and pressures, once the impactor is operated with the same critical orifice.
- The critical Stokes number is independent of atmospheric temperatures and pressures.
- The impactor is laid out for air. Viscosities and acoustic velocities are well tabulated for a wide temperature range. The ratios of specific heats and the mean free paths can be easily derived for the same range of temperatures.

Rather large uncertainties are associated with the values of correction coefficients which take the shape of the orifices into account. Effects of internal friction and friction with the walls are rather low, once the thickness of an orifice is small compared to its aperture. However, the coefficient of contraction may depend on the size of the orifice. In other words, specific investigations into the coefficients of contraction for the small orifices used in the HT-LPI would be needed. Listed values of $C_c \approx 0.62$ are good for a start, but are probably subject to changes.

The Cunningham slip correction factor is subject to uncertainties. The dependence of the factors on medium and material of particles is not well known, nor their dependence on temperatures and pressures.

An experimental calibration of the HT-LPI at high temperatures, a very interesting project by itself, is beyond the scope of the current work. It is feasible but expensive to measure operational data of a proper instrument at high temperatures up to 1,000°C. It is certainly beyond the state-of-the-art to prepare a suitable test aerosol for highest temperatures and to characterize it at these conditions.

5.4 DESIGN, CALIBRATION AND VALIDITY CHECK OF THE HT-LPI

5.4.1 Comparison of the design data with data from tests at cold conditions

A set of orifice plates of the HT-LPI used during the test runs mentioned in section 6 has been investigated concerning the size of the orifices and the pressure ratios in the stages. The sizes are measured in a microscope. The pressure ratios were determined in special stage casings facilitating measurements of the inter-stage pressures. The experimental data sets were completed by the volumetric flow rate V_a of the HT-LPI impactor at atmospheric temperature T_a and pressure P_a.

Geometry and size of the orifices

The orifices are made by laser technology. As a consequence the orifices are not perfectly round. They are random ovals, occasionally with a well determined eccentricity. Moreover, the material is partly not removed from the apertures. Droplets on the edges of orifices are frequently observed.

In Table 1 the measured orifice sizes of the HT-LPI stages are compared to the nominal sizes used during the lay-out of the impactor. The actual diameters of the fine orifices differ considerably from the nominal diameters. A more accurate determination is under way. As all orifices of the fine stages increase in size by about the same factor the effect on the impactor would be an increase of the volumetric flow rate, but not an increase of the jet velocities.

Table 1: Comparison of nominal and actual equivalent diameters of the orifices

Stage number	1	2	3	4	5	6	7	8
nominal diameter [mm]	0.315	0.315	0.315	0.375	0.500	0.750	1.130	1.750
actual diameter [mm]	0.327	0.339	0.335	0.411	0.497	0.734	1.132	1.765

Table 2: Jet velocities for nominal and actual orifice diameters of the HT-LPI at ambient conditions

Explanation: ambient conditions : $T_a = 20°C$; $P_a = 1{,}013.25$ mbar

Stage number	1	2	3	4	5	6	7	8
nominal velocity [m/s]	285	212	134	83.5	50.5	31.1	17.6	7.75
actual velocity [m/s]	297	217	139	82.5	60.0	37.5	14.4	8.77

Ratios of the inter-stage pressures

As listed in Table 3 the inter-stage pressure ratios which determine the operational state of the impactor do not differ very much in the fine stages. The differences are not important, as is also indicated by the jet velocities listed in Table 2.

Table 3: Comparison of nominal and actual inter-stage pressure ratios

Stage number	1	2	3	4	5	6	7	8
nominal ratio	0.657	0.780	0.904	0.976	0.986	0.995	0.998	0.999
actual ratio	0.634	0.794	0.911	0.966	0.989	0.992	0.998	0.999

Volumetric flow rates

There is an increase of the nominal volumetric flow rate, V = 7.63 l/min to the actual volumetric flow rate, V = 10.05 l/min, at standard temperature T_o = 20°C. This increase by about 37 % is largely explained by the form of the critical orifice. In the lay-out the critical orifice was supposed to be a large hole of about 1.6 mm in a lamina of 0.1 mm thickness. The contraction factor would be C_c = 0.62. However, due to constructive reasons the orifice was drilled into a lamina of about 1 mm thickness. This is already sufficient for the flow to form a vena contracta inside the orifice and a turbulent break down of the flow which now fills the cross section completely. Volumetric flow rates are proportional to the acoustic velocity which is the same in both cases. For a thin orifice the volumetric flow rate would be given by $V_{thin} = A_o \cdot 0.62$, in the thick orifice the volumetric flow rate is given by $V_{thick} = U_a \cdot A_o \cdot 0.80$. This means an increase by about 34 % (A_o: area of the orifice).

This increase of the flow rates is compensated by an increase of the diameters of the orifices and by an increase of the effective contraction coefficient of the jets, $C_c \approx 0.75$ instead of $C_c \approx 0.62$. So the inter-stage pressure ratios are affected only marginally. The increase of the orifice diameters and the increase of the contraction coefficient shift the cut-sizes to larger diameters, however.

Comparison of cut-sizes

Finally the calibrations of the HT-LPI impactor for different temperatures were compared (see Figure 2). The calibrations based on the actual experimental data (volumetric flow rate, inter-stage pressure ratios) are shifted to larger sizes due to the larger orifices and larger contraction coefficients.

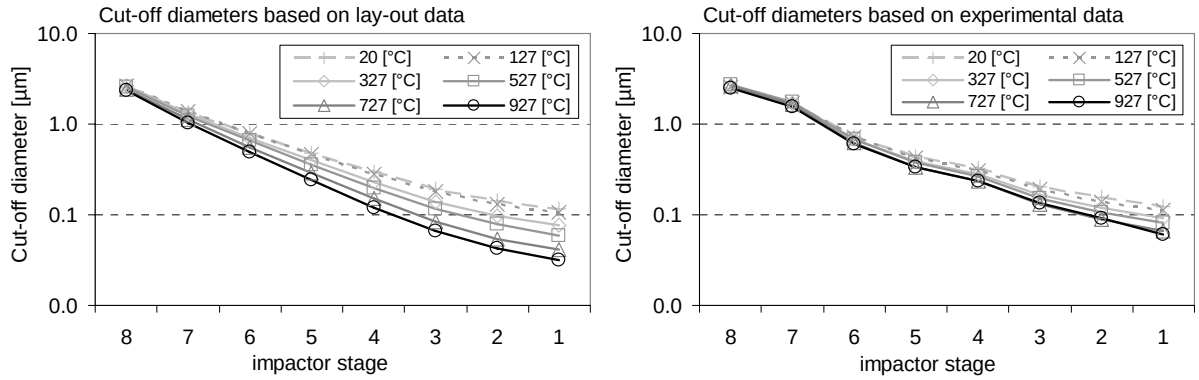

Figure 2: Calculated calibration of the HT-LPI for different ambient temperatures

5.4.2 Validity check

The aim was to check the whole system concerning leakage problems and to compare measurement results gained with the HT-LPI with results from BLPI measurements. Therefore, the HT-LPI was tested at cold gas conditions (200°C) during test runs with wood chips (softwood) at boiler outlet of a 180 kW_{th} grate fired combustion unit. At the same sampling position measurements with a conventional 9-stage BLPI have been performed.

As shown in Figure 3 the particle size distributions of aerosols sampled with the HT-LPI show similar characteristics as those sampled with a conventional BLPI. However, as it can be seen in Figure 2 the cut-off diameter of the smallest HT-LPI stage at this low temperature range is above 0.1 µm. Moreover, contrary to the BLPI the HT-LPI is not equipped with a backup filter and therefore a comparison of the total mass of particles < 1 µm (ae.d.) sampled with the different impactors can not be performed. Instead the total mass of particles in a comparable size range has been accounted. Four HT-LPI measurements as well as four BLPI measurements have been considered for these evaluations. The mean mass concentration of particles in the size range of 0.18 – 1 µm (logarithmic mean of the aerodynamic particle diameter) determined with the BLPI was 11.9 mg/Nm³. The mass of particles sampled in the size range of 0.16 – 1.11 µm (logarithmic mean of the aerodynamic particle diameter) during HT-LPI measurements was 11.2 mg/Nm³. Considering the different size ranges and the fact that aerosol emissions in a biomass combustion unit always show certain fluctuations, these results are well comparable. It is foreseen to repeat test runs with HT-LPI and BLPI measurements downstream the boiler in certain intervals in order to check, if due to the operation of the HT-LPI at high temperatures changes concerning its operation occur. Such changes could be caused by minor deformations especially of the orifices.

The second method applied to check the plausibility of the measurement results was to comprehensively analyze the results of SEM-analyses of particle samples taken with the HT-LPI at high temperatures. The shape of the

particle depositions on the precipitation foils for instance was analyzed in order to gain information about the diameter of the jet leaving the orifice. Moreover, the particle size of single particles was determined and the data were compared with the cut-off diameters of the respective impactor stages. Additionally, particle depositions which were found apart from the main deposition peaks were analyzed in order to gain information about the detailed flow conditions in the impactor stages. Summing up the results of these investigations it can be stated, that they resemble the classical flow and particle behavior which is usually determined for low pressure impactors.

Based on these tests two important conclusions concerning the operation of the HT-LPI can be drawn.

- The particle size distributions determined with the HT-LPI during cold gas measurements are comparable with particle size distributions measured with a conventional BLPI. Also SEM-analyses of particles sampled on the single impactor stages showed no major deviations concerning particle sizes precipitated in the different stages compared with the impactor design. Therefore, it can be assumed, that the concept chosen concerning orifice diameters, stage thickness and stage design works properly.
- The mass of particles in a certain size range determined with the HT-LPI is comparable with the one determined with the conventional BLPI. This leads to the conclusion, that the impactor design chosen is air tight and that no leakage flows occur.

Consequently, the new impactor concept had proven its applicability for low-temperature measurements and was ready for an application during high temperature particle measurements.

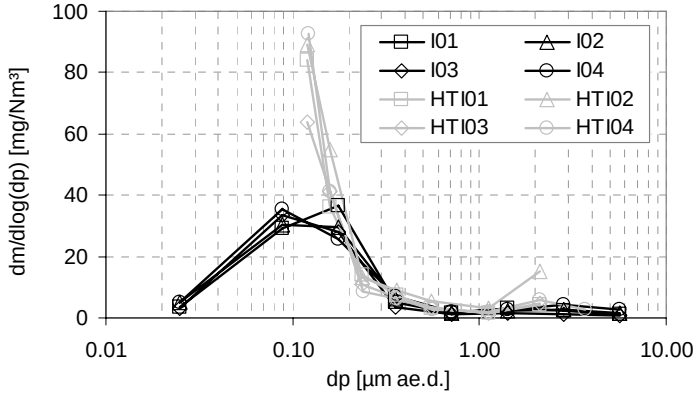

Figure 3: Comparison of particle size distributions of aerosols at boiler outlet measured with a BLPI as well as with a HT-LPI

Explanations: all concentrations related to dry flue gas and 13 vol.% O_2; ae.d. … aerodynamic diameter

6 Application of the HT-LPI

The HT-LPI has up to now successfully been applied during test runs at a 440 kW_{th} pilot-scale combustion unit equipped with a hot water boiler firing three different biomass fuels (wood chips, bark, waste wood), during test runs at two large-scale grate-fired biomass combustion plants utilizing waste wood respectively straw as fuels (water tube steam boilers) as well as at a power station co-firing sawdust and coal (220 MW_{el}; pulverized fuel combustion). In this paper results determined during test runs at a waste wood fired large-scale CHP-plant are presented as an example for the application of the new measurement and sampling device.

6.1 DESCRIPTION OF THE PLANT

The nominal boiler capacity of the waste wood fired CHP-plant is 44 MW_{th} (steam parameters: 66 bar, 452°C). The flue gas is cleaned by a double cyclone and a baghouse filter, SNCR is applied for NO_x reduction and a dry sorption system is applied for HCl, SO_x and PCDD/F-emission control. The combustion unit was operated at approximately 90% of nominal boiler load during almost the whole duration of the test run.

The waste wood used was of quality A1 to A4 according to German quality standards (RAL Deutsches Institut für Gütesicherung und Kennzeichnung e.V., 1997). A characterization of the fuel is given in Table .

Table 4: Characterization of the waste wood (quality A1-A4) used during the test run

Explanations: m.c. … moisture content; d.b. … dry base; w.b. … wet base; mean, s … mean value and standard deviation based on 3 fuel analyses

	m.c. [wt% (w.b.)]	ash [wt% (d.b.)]	Ca	Si	K	Na	Zn	Pb	S	Cl
			[mg/kg (d.b.)]							
mean	27.2	16.4	8,289	46,657	2,543	2,707	794	141	1,503	1,195
s	3.4	2.3	1,028	8,646	162	495	352	22	223	275

HT-LPI measurements were performed at three different sampling points, situated in the first duct of the boiler, the second duct and downstream the first superheater in the third duct. Moreover, BLPI measurements at boiler outlet (downstream the economizer) have been performed (see Figure 4). By the evaluation of the measurement results it is possible to investigate the formation of aerosols in dependence of the decreasing flue gas temperature under real-scale conditions.

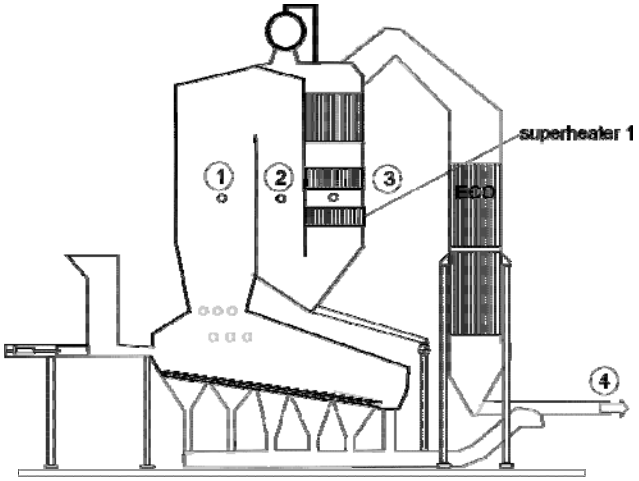

Figure 4: Scheme of the waste wood fired CHP plant and measurement positions where HT-LPI and BLPI measurements took place

Explanation: ECO … economizer; HT-LPI measurements: 1: 1st duct of the boiler; 2: 2nd duct of the boiler; 3: downstream superheater 1; BLPI measurements: 4: downstream economizer

6.2 RESULTS AND DISCUSSION

Concerning aerosol formation during fixed-bed combustion of waste wood, Obernberger et al. (2001) propose the following process. Waste wood is, compared with other biomass fuels, extremely Zn-rich (see also Table). Under reducing conditions, as they usually prevail in the gasification zone of a grate-fired combustion unit, Zn is released as elemental Zn to the gas phase, subsequently is oxidized and immediately forms submicron particles. Later on, during the cooling of the flue gas, alkaline metal chlorides and sulfates as well as Pb-compounds (chlorides and/or oxides) start to condense and either form new particles by nucleation or condense on the surfaces of the already existing ZnO particles. If the number concentration of the ZnO particles is high enough further nucleation is suppressed and condensation of ash forming vapors on the surfaces of the ZnO particles is the dominating mechanism. Moreover, coagulation of particles leads to particle growth.

In Figure 5 the mean particle size distributions (PSD) of aerosols sampled at the four different sampling points outlined are shown. For aerosols sampled in the 1st duct as well as in the 2nd duct of the boiler the peak in the PSD has been identified at a particle diameter of 0.3 µm (ae.d.), whereas the peak diameter of aerosols sampled downstream the first superheater is situated slightly above 0.2 µm (ae.d.). Aerosols sampled at boiler outlet with a conventional BLPI showed a clear peak diameter of approximately 0.35 µm (ae.d.).

Also the concentrations of aerosols detected at the four sampling points as well as the temperatures measured at the sampling points are summarized in Figure 5. Considering the average aerosol emission of 87.8 mg/Nm³ measured at the boiler outlet, it can be stated that about 67% of the aerosols already existed in the first duct of the furnace, about 50-80% after the second duct and between 60-95% downstream the first superheater. Consequently, 5-40% of the aerosol forming species are still in the gaseous phase at temperatures of about 400°C.

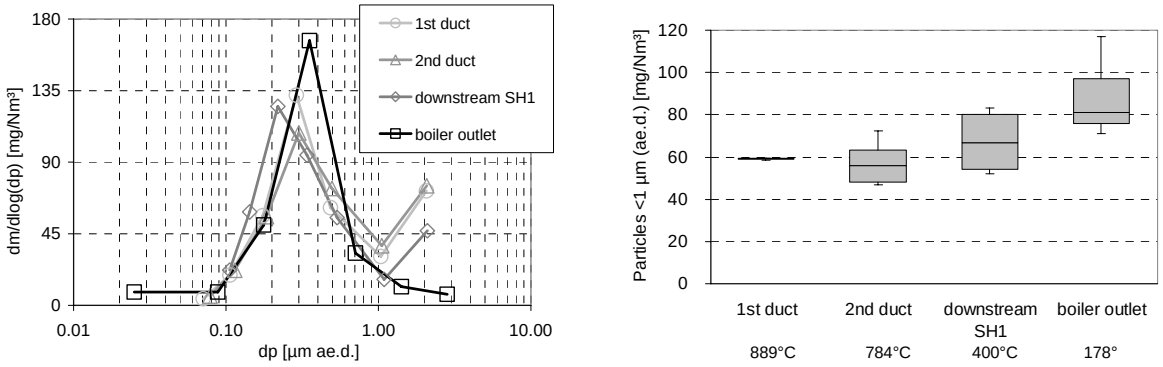

Figure 5: Mean particle size distributions as well as concentrations of aerosols at 4 different sampling points

Explanations: all concentrations related to dry flue gas and 13 vol.% O_2; ae.d.: aerodynamic diameter; the boxes indicate the quartiles 25% to 75%, the line in the box displays the median value, furthermore maximum and minimum values are shown; number of measurements performed: 1st duct: 2; 2nd duct: 5; downstream SH1: 4; boiler outlet: 6; mean flue gas temperatures calculated from all measurements performed at a the respective sampling port; flue gas temperatures for 1st and 2nd duct measured with a suction pyrometer; since no temperature measurement downstream SH1 was possible the flue gas temperatures were estimated based on the steam temperatures; flue gas temperature at boiler outlet recorded by process control system (thermocouple)

The increasing aerosol concentration in the flue gas with decreasing temperature is an expected result, however, which compounds are responsible for aerosol formation in the different sections of the furnace and the boiler can be revealed by the evaluation of the results gained from SEM/EDX analyses of the HT-LPI samples. The results of these analyses are summarized in Table 5. Moreover, results from wet chemical analyses of BLPI-samples taken downstream the economizer are presented.

Table 5: Chemical composition of aerosols sampled at high temperatures directly from the boiler, downstream the first superheater as well as downstream the economizer

Explanations: measurements performed at mean flue gas temperatures of 907°C (1st duct), 802°C (2nd duct), 400°C (after superheater 1 … SH1) and 164°C (downstream economizer); HT-LPI analyses by SEM/EDX; results normalized to 100% not considering Pt (material of sampling foil), Cr (component of the alloy of stainless steel 1.4841) and C (used for coating of the sample); O calculated; detection limit for EDX-analyses: 1 wt%; BLPI: wet chemical analyses; Al not detectable due to Al-sampling foils; O calculated

	Ca	Si	Mg	K	Na	Zn	Mn	Pb	S	Cl	P	Ti	Fe	Al	O
	wt%	wt%	wt%	wt%	wt%	wt%	wt%	wt%	wt%	wt%	wt%	wt%	wt%	wt%	wt%
1st duct	< 1	1.5	< 1	15.1	8.2	25.1	< 1	3.1	12.6	0.0	< 1	< 1	< 1	< 1	33.4
2nd duct	< 1	2.3	< 1	7.2	6.3	42.9	< 1	2.7	7.2	0.0	< 1	< 1	< 1	< 1	29.1
after SH1	< 1	2.1	< 1	15.1	5.7	26.2	< 1	5.3	8.7	6.2	< 1	< 1	< 1	< 1	27.6
after ECO	< 1	1.4	< 1	11.3	4.4	27.3	< 1	4.2	5.2	17.5	< 1	< 1	< 1	n.d.	17.1

Aerosols sampled in the 1st duct of the boiler mainly consist of Zn, K, Na and S. Moreover, considerable amounts of Pb and Si have been identified in the smaller particles. Aerosols sampled in the 2nd duct of the boiler again mainly consist of Zn, K, Na and S. The concentrations are shifted to higher Zn concentrations. Considering the fuel data presented in Table 4, which indicate an average Zn content of 794 mg/kg (d.b.) and an extremely high standard deviation of 352 (relative standard deviation: 44%), the higher Zn-concentrations in the second duct may be due to inhomogeneities of the fuel. At the third measurement point downstream superheater 1 increased Cl and Pb concentrations indicate the enforced condensation of Pb and Cl-compounds during the cooling of the flue gas. A further increase of the Cl-concentrations in the particles takes place in the remaining boiler and economizer sections.

The HT-LPI-measurements performed give an exciting insight into aerosol formation during the cooling of the flue gas in a steam boiler. In Figure 6 the concentrations of elements calculated from the flue gas data, the HT-LPI measurements and the BLPI measurements downstream the economizer are summarized which provide the opportunity to follow particle formation for the elements considered along the pathway of the flue gas through the radiative and the convective path. In this context it has to be mentioned, that HT-LPI measurements are rather time consuming. Especially the cooling of the impactor after the measurement takes more than two hours and therefore a considerable period of time (some hours) is necessary between two measurements. The inhomogeneity of the fuel (see Table 4) can therefore influence the results. However, the comparison of the data

gained from the measurements in the different sections still gives good indications about the main processes governing aerosol formation.

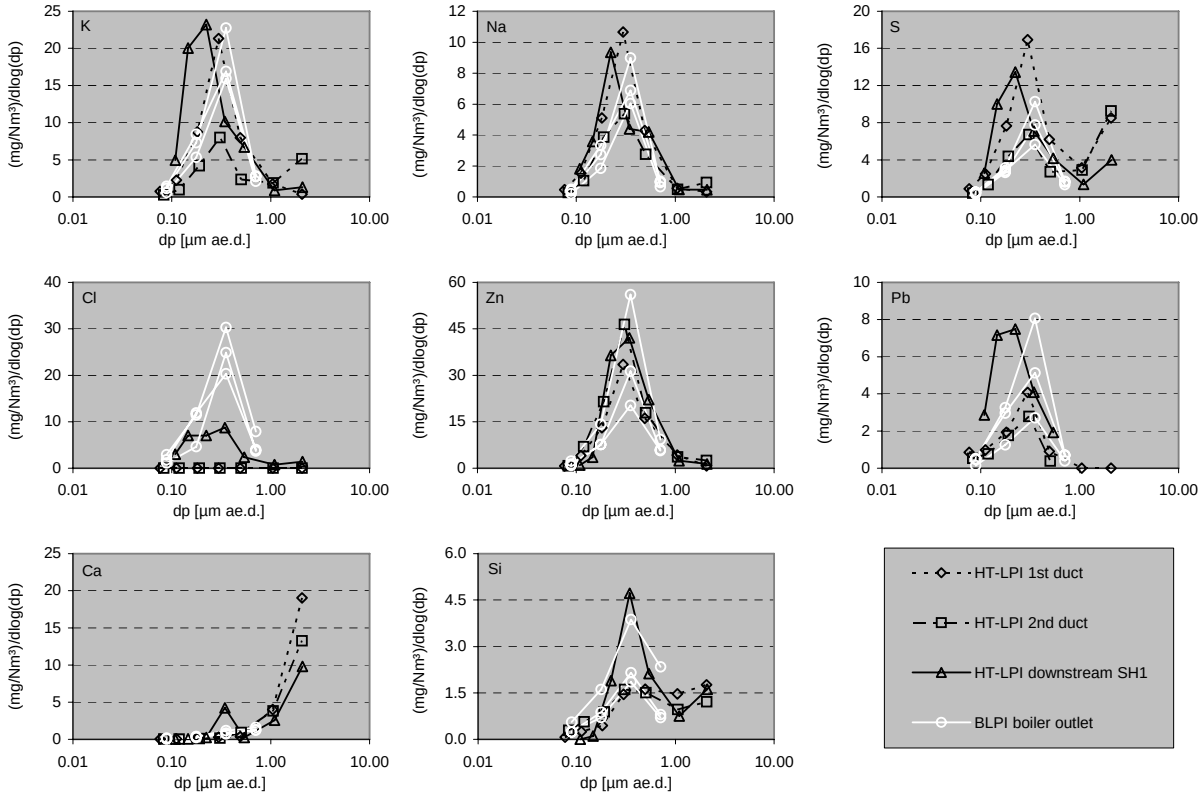

Figure 6: Concentrations of particle bound elements in the flue gas at boiler outlet and in the 3 ducts of the combustion unit

Explanations: all concentrations related to dry flue gas and 13 vol.% O_2; ae.d.: aerodynamic diameter; SH1: superheater 1

As already mentioned, Zn, K, Na, S and Pb are the most relevant constituents of the aerosols sampled in the first duct. ZnO is the first component which is supposed to undergo gas to particle conversion. This process has already been observed during test runs at another waste wood fired combustion plant. Analyses of particles sampled during these test runs on a quartz filter upstream the boiler have revealed, that mainly ZnO particles are formed at high temperatures (Brunner et al., 2004). This formation of ZnO particles in a size range of some nanometers is assumed to take place directly after the flue gas leaves the fuel bed. Afterwards coagulation leads to particle growth which is confirmed by the fact that the Zn distribution in the aerosols follows the shape of the particle size distribution. In Figure 7 a SEM image and EDX-analyses of such ZnO particles on which alkaline metal sulphates have condensed, are presented. The image shows almost spherically shaped particles. The molar composition gained from the EDX-analyses indicates that the particles consist of ZnO, K_2SO_4, Na_2SO_4 and small amounts of SiO_2.

2^{nd} duct – stage 2 d50 = 0.09 µm

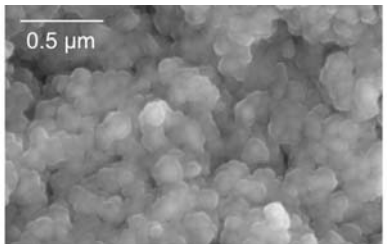

	mole%	weight %
Ca	< 1.0	<1.0
Si	3.8	3.5
Mg	< 1.0	<1.0
K	4.8	6.0
Na	6.1	4.5
Zn	20.3	43.1
S	6.4	6.6
P	< 1.0	<1.0
Ti	< 1.0	<1.0
Fe	< 1.0	<1.0
Al	< 1.0	<1.0
Pb	< 1.0	5.1
O	56.3	29.1

Figure 7: SEM-image and EDX-spectra of aerosols sampled in the 2^{nd} duct of the boiler

Explanations: primary electron energy: 12 keV; O is calculated; due to C-coating C was not considered

By calculating the molar concentrations of the elements K, Na, Pb and S in the aerosols from the mass related data provided in Table 5, it can be revealed that almost exactly the amount of S is available to bind all the K, Na and Pb as sulphates. From the thermodynamic data of K_2SO_4 and Na_2SO_4 it can be calculated, that the saturation vapour pressures of these compounds at temperature prevailing during the particle sampling (907°C) amount to approximately 0.036 Pa respectively 0.009 Pa. If only the K_2SO_4 and Na_2SO_4 determined in the aerosol fraction in the first duct is considered, partial pressures in the gas phase prior to gas to particle conversion of approximately 0.4 Pa respectively 0.3 Pa can be calculated for these compounds. The actual gas phase concentrations are even higher since the amount of K_2SO_4 and Na_2SO_4 which has not condensed yet is not considered. However, this rough estimation clearly shows that saturation has already been exceeded before sampling point 1 and therefore, the presence of K_2SO_4 and Na_2SO_4 containing particles is thermodynamically plausible. Concerning $PbSO_4$ these estimations could not be performed, since no reliable thermodynamic data are available. However, the melting point of $PbSO_4$ amounts to 1,170°C and therefore also the formation of solid $PbSO_4$ seems reasonable.

Comparing the results of the EDX-analyses of particles sampled in the 1st and the 2nd duct, higher particle bound Zn-concentrations and lower particle bound K, Na and S concentrations are obvious. Since the temperature decrease form 907 to 802°C can not explain the increase of the Zn-concentrations and since there is also no plausible reason for the decrease of the concentrations of the other elements mentioned, fuel inhomogeneities seem to be responsible for these effects.

Between sampling point 2 and sampling point 3 the flue gas is cooled from 802°C to approximately 400°C. Due to the decreasing temperatures also significant changes concerning the compounds which undergo gas to particle conversion occur. Mainly for K and Pb significant increases of their particle bound concentrations in the flue gas must be mentioned. Moreover it can be seen, that at these decreasing temperatures chlorides start to play a major role instead of sulphates. The analyses data clearly show, that the amount of Cl available in the particles sampled downstream the superheater is sufficient to bind all the K and Pb which is not bound as sulphate. Even a small amount of excess Cl is available which may indicate the formation of $ZnCl_2$.

Concerning the formation of KCl, the comparison with thermodynamic data proves the plausibility of results. Assuming as an extreme case, that all the Cl detected in the particles sampled at measurement point 3 (downstream superheater) is bound as KCl a gas phase concentration of KCl of about 17 mg/Nm³ or 5.02 ppm corresponding to a vapour pressure of 0.5 Pa can be calculated. Saturation for this KCl concentration in the flue gas is reached at about 610°C which represents a temperature between duct 2 (about 800°C) and superheater outlet (about 400°C). Assuming as a second extreme case that all the Pb detected in the particles sampled with the HT-LPI at sampling point 3 is bound as $PbCl_2$, the KCl concentration drops to approximately 12 mg/Nm³ and therefore gas/solid equilibrium is reached at 600°C. Consequently, it is plausible that KCl particles are formed in the superheater region. The same calculations can also be performed for $PbCl_2$ and $ZnCl_2$. The results also indicate that the formation of solid $ZnCl_2$ and $PbCl_2$ in the superheater 1 and downstream superheater 1 is thermodynamically possible.

Comparing the element concentrations in the aerosols at superheater outlet (sampling point 3) with the data gained from the analyses of submicron particles sampled downstream the economiser, obviously further condensation of Cl-containing compounds takes place. However, the data gained from the analyses of aerosols sampled downstream the boiler scatter due to inhomogeneities of the fuel, and therefore, no clear conclusions concerning the exact shares of Zn, K and Pb chlorides which condense in the economiser section can be drawn. It has additionally to be considered, that direct condensation on heat exchanger surfaces also reduces the concentrations of ash forming vapours in the flue gas.

Submicron Ca and Si particles are, due to their low volatility, expected to be entrained directly from the fuel bed. As a main mechanism therefore the fragmentation of Ca and Si structures embedded in the fuel matrix is proposed (Brunner et al., 2004). Therefore, Ca and Si particle formation takes places upstream the first measurement point and consequently, the particle bound concentrations of these elements in the flue gas should be in the same range for all measurement points. However, the formation of Ca particles in and downstream superheater 1 is indicated by the analyses of the 4th HT-LPI stage of the impactor sample taken downstream superheater 1. This should be taken as an outlier, which might be due to the broad variations in the fuel composition of waste wood. The results for Si could also indicate the formation of Si-particles in the superheater region. On the other side the fuel data presented in Table 4 show a high standard deviation for Si and the broad variation of particle bound Si in the flue gas at economiser outlet underlines the influence of the varying Si-contents of the fuel on Si particle formation. Therefore, the significantly increased particle bound Si-concentration in the flue gas determined during the measurement downstream superheater 1 is supposed to be due to the inhomogeneity of the fuel.

7 Conclusions and outlook

In this paper the development of a high-temperature low-pressure impactor (HT-LPI) that can be applied in furnaces at temperatures up to 1,000°C has been described and first results from measurements with this impactor have been presented.

The selection of the materials applied to manufacture the HT-LPI has been a crucial step of the work performed. It can generally be concluded that the materials chosen have proven their applicability for the special high temperature requirements.

The results of measurements performed at boiler outlet of a biomass combustion plant showed that the PSD determined with the HT-LPI is comparable with the PSD measured with a conventional BLPI at the same sampling point. Also SEM-analyses of particles sampled on the single impactor stages showed no major deviation concerning their actual particle size compared with the impactor design. Therefore, it can be assumed, that the concept chosen concerning orifice diameters, plate thickness and stage design works properly. Moreover, the mass of particles in a certain size range determined with the HT-LPI is comparable with the one determined with the conventional BLPI. This leads to the conclusion, that the impactor is air tight and that no leakage flows occur.

Concerning the calibration of the HT-LPI it is intended to perform an additional experimental calibration of one or two impactor stages. The steepness of the precipitation efficiency curve is thus of special interest. Due to the thin orifices used for the HT-LPI lower turbulence in the jet might prevail and thus would lead to better precipitation efficiency curves than for other orifice designs. However, this hypothesis is not yet proven.

Moreover, it can be stated that a comparison of nominal orifice diameters with actual orifice diameters showed discrepancies which are caused by the laser technology used for the drilling of the orifices. Besides that a higher actual effective contraction coefficient of the jets has been determined compared to the nominal effective contraction coefficient. Both the increase of the orifice diameters and the increase of the contraction coefficient shift the cut-sizes to larger diameters. Currently a new approach for laser-drilling the orifices applying a newly developed micro processing facility is in the test phase. The results of first test drillings are encouraging. The influence of more precise orifices on the calibration of the impactor will subsequently be evaluated.

The HT-LPI has successfully been applied during test runs at a pilot-scale combustion unit firing three different fuels (wood chips, bark, waste wood) and during large-scale grate-fired biomass combustion plants firing waste wood and straw as well as at a large-scale power station co-firing coal and sawdust. The following conclusions concerning the application of the HT-LPI for the investigation of aerosol formation during large-scale combustion of waste wood can be derived from the data presented in this paper.

The HT-LPI-measurements performed enable an exciting insight into aerosol formation during the cooling of the flue gas in a steam boiler. By comparing the results of HT-LPI measurements in the first duct and the second duct of the boiler, downstream the first superheater as well as BLPI measurements downstream the economizer, the particle formation process can be followed. It has for instance been shown, that about 67 wt% of the particle emission measured at boiler outlet, already exists in the first duct. This share increases to up to 95 wt.% downstream the superheater. Moreover, the application of SEM/EDX-analyses on the samples gained from the impactors provides the possibility to analyze aerosol formation on an element basis. It has for instance been shown that during the combustion of waste wood ZnO particles are the first to be formed. Later on, during the cooling of the flue gas in the radiative and the convective path of the plant, alkaline metal sulfates and chlorides as well as $PbSO_4$ and $PbCl_2$ undergo gas to particle conversion processes.

Summing up, it can be stated, that with the HT-LPI a unique particle sampling device has been developed which opens new possibilities concerning ash and aerosol related research in combustion processes. The present design of the HT-LPI works with a sufficient accuracy, however, in order to improve this accuracy and to further prove the results gained from the measurements, additional optimization measures and calibration work are planned to be performed in the coming months.

8 Acknowledgements

The research is supported by the European Commission under Contract SES-CT-2003-502679, “BIOASH”.

9 References

Bohl, W., 1971, Technische Ströhmungslehre. Vogel-Verlag, Würzburg.

Brunner T., Jöller M., Obernberger I., 2004, Aerosol formation in fixed-bed biomass furnaces - results from measurements and modelling. In: Proc. of the Internat. Conf. Science in Thermal and Chemical Biomass Conversion, Sept 2004, Victoria, Canada, ISBN 1-872691-97-8, pp.1-20, CPL Press (Ed.)

Dixkens, J., Fissan, H., 1995, Development of a ceramic-cascade-impactor for size classified particle sampling in high pressure- and high temperature-(HPHT)processes. J. Staub – Reinhaltung der Luft 55, 283-291.

Doughertý, R.L., Franzini, J.B., 1977, Fluid Mechanics with Engineering Applications. 7th ed. McGraw Hill Book Company.

Jimenez, S., Ballester, J., 2005, A Comparative Study of Different Methods for the Sampling of High Temperature Combustion Aerosols. J. Aerosol Science and Technology 39, 811-821.

Kröpfl, P., Berner, A.,. Reischl, G.P., 2003, On the calibration of Berner low-pressure impactors. J. Aerosol Science, Special issue: Abstracts of the European Aerosol Conference 2003, S1239-1240.

Obernberger, I., Brunner, T., Joeller, M., 2001, Characterisation and Formation of Aerosols and Fly-ashes from Fixed-bed Biomass Combustion, in Nussbaumer, T., (Ed.), Aerosols from Biomass Combustion, International Seminar at 27 June in Zurich by IEA Bioenergy Task 32 and Swiss Federal Office of Energy, Verenum, Zurich, pp.69-74.

RAL Deutsches Institut für Gütesicherung und Kennzeichnung e.V., 1997, Gütesicherung RAL-GZ 428: "Recyclingprodukte aus Gebrauchtholz". Beuth-Verlag, Berlin, Germany.

Strand, M., Boghard, M., Swietlicki, E., Gharibi, A., Sanati, M., 2004, Laboratory and Field Test of a Sampling Method for Characterisation of Combustion Aerosols at High Temperatures. J. Aerosol Science and Technology 38, 757-765.